

# Uptake of Organic Pollutants by Silica—Polycation-Immobilized Micelles for Groundwater Remediation

Yael G. Mishael and Paul L. Dubin\*

Department of Chemistry, Indiana University—Purdue University, 402 North Blackford Street, Indianapolis, Indiana 46202

Interest has grown in designing new materials for groundwater treatment via “permeable reactive barriers”. In the present case, a model siliceous surface, controlled pore glass (CPG), was treated with a polycation (quaternized polyvinyl pyridine, QPVP) which immobilizes anionic/nonionic mixed micelles, in order to solubilize a variety of hydrophobic pollutants. Polymer adsorption on CPG showed atypically slow kinetics and linear adsorption isotherms, which may be a consequence of the substrate porosity. The highest toluene solubilization efficiency was achieved for the silica—polycation-immobilized micelles (SPIM) with the highest polymer loading and lowest micelle binding, a result discussed in terms of the configuration of the bound polymer and the corresponding state of the bound micelles. The ability of SPIM to treat simultaneously a wide range of pollutants and reduce their concentration in solution by 20–90% was demonstrated. Optimization of SPIM systems for remediation calls for a better understanding of both the local environment of the bound micelles and their intrinsic affinities for different hydrophobic pollutants.

## Introduction

Permeable reactive barriers (PRBs) constitute a relatively new approach for the in situ remediation of polluted groundwater (1, 2). Over 90 PRBs are applied around the globe including the U.S., Europe, Japan, and Australia (3). Their use in North America began in the mid-1990s and focused on the treatment of relatively simple mixtures of chlorinated solvents with zero-valency barrier systems (4). Recognizing the success and remediation potential of PRBs, the U.K. Environmental Agency proposed new guidelines that are broad in scope and cover both a wide range of barrier designs and target pollutants (5). This variety of approaches is reflected in the diversity of materials proposed for use in PRBs including (in addition to zero-valent metals) humic materials, oxides, ion-exchange resins (6), iron minerals, activated carbon, and oxygen- and nitrate-releasing compounds (1). Surfactant-modified PRB materials, such as modified soils (7), clays (8), natural minerals (9), and polymer-modified silica (10), belong to a class of substances for which efficacy is based on partitioning of nonpolar organic pollutants into the modified surfaces (2). Recently, a novel filter based on sand and micelle-modified clay (100/1 w/w) for water treatment from organic

pollutants was reported (11). The efficiency of this filter to remove 94–99% of the initial concentration of several herbicides was demonstrated.

The partitioning of pollutants into surfactant micelles as a means of water and soil remediation has been extensively reported. With the goal of improving the understanding of this class of techniques, partition coefficients have been calculated for several pollutants (12–17). Such information is directly relevant to micellar-enhanced ultrafiltration, which remediates water by forcing it through an ultrafiltration membrane with pore sizes small enough to block passage of the micelles and associated pollutant (18, 19). However, most development and field tests related to surfactants throughout the past decade have focused on “enhanced pump and treat” (20–22). These solubilization-based techniques engender large volumes and therefore entail additional procedures to immobilize the solubilized pollutants. Thus, a procedure that combines surfactant-based solubilization with immobilization would be of interest.

The adsorption of polycations on negative surfaces has been studied intensively and is reasonably well understood (23). Studies of complexation between polycations and negatively charged micelles have received considerable attention as well (24). The structure of the micelles in the polyelectrolyte–micelle complexes is still to be unraveled but CryoTEM (25) and solubilization results (26) suggest that complexation involves little perturbation of the micelle structure. While relatively few studies have addressed the coadsorption of polymers and surfactants (27–29), Aloulou et al. (30) reported the retention of organic solute on cellulose fibers treated with polycation and anionic surfactant. In a related area, it was observed that a polycation adsorbed on glass shows the same protein-binding selectivity as does the free polycation (31). Taken together, these results suggest that negatively charged micelles immobilized by polycations to a silica surface may retain their solubilizing powers.

In our previous report we demonstrated the principle of binding an anionic micelle to a negatively charged surface via a cationic polymer in order to achieve immobilized detergency with the goal of removing hydrophobic solutes from an aqueous phase. In particular poly(dimethyldiallylammonium chloride) was used to bind SDS/TX100 anionic/nonionic mixed micelles to both sand and controlled pore glass (a commercially available material with well-characterized surface and pore properties, well-known as a chromatographic support). The resultant silica/polyelectrolyte-immobilized micelle (SPIM) was shown to solubilize a hydrophobic dye (32), suggesting its utilization in a PRB. In the current work, we investigate two issues. (1) First, we explore the interrelationship between polyelectrolyte adsorption, micelle binding and solubilization of organic pollutants in the micelles by examining how ionic strength and polymer concentration in polycation adsorption influence micelle loading and uptake of a model pollutant, toluene. (2) The expectations from the previous work are additionally fortified by measurements of the removal of “real pollutants”, and we demonstrate simultaneous uptake from solution by SPIM of a mixture of two-dozen halocarbon and aromatic compounds. The results indicate the central role of the configuration of the bound polymer and should facilitate incorporation of SPIM in a variety of water remediation applications including PRBs and filtration systems, along the lines recently described in ref 11.

\* Corresponding author phone: (413)577-4167; e-mail: dubin@chem.umass.edu.

## Materials and Methods

**Materials.** Poly-4-vinylpyridine quaternized with methyl iodide (QPVP) was "Reilline 450 quat" from Reilly Industries (Indianapolis, IN). Sodium dodecyl sulfate (SDS) was purchased from Fisher Scientific (FairLawn, NJ). Triton X-100 (TX100), toluene, and acetonitrile were from Aldrich (Milwaukee, WI). Standard purgeable halocarbon and aromatics mixtures were from ULTRA Scientific (North Kingstown, RI). Milli-Q water was used throughout this study. Controlled pore glass (CPG) (particle size of 75–125  $\mu\text{m}$ ) with a mean pore diameter of 7.5 nm ( $\pm 20\%$ ) and a surface area of 153  $\text{m}^2/\text{g}$  was purchased from Millipore (Lincoln Park, NJ). This pore size was chosen on the basis of its large surface area; however, a remarkable finding (see below) was the efficient adsorption on this CPG of a polycation with a hydrodynamic radius larger than the pore radius. The CPG was washed for 1 h in a 1% SDS, pH 9.5, NaOH solution, then rinsed with Milli-Q water and dried at 50  $^\circ\text{C}$  overnight.

**Dynamic Light Scattering (DLS).** Solutions of TX100/SDS (20 mM,  $Y = 0.35$ ) and QPVP (5 g/L) (pH = 9.5 and NaCl = 0.5 M) were prepared. DLS measurements were made after sample filtration (0.2  $\mu\text{m}$ ) using a Malvern Instruments (Southborough, MA) Zetasizer Nanosystem SZ. Mean apparent translational diffusion coefficients ( $D$ ) were determined by fitting the autocorrelation functions using with the program "general modes", similar to CONTIN, and the apparent hydrodynamic radii were calculated from Stokes law.

**Turbidimetric Titration.** Turbidity measurements were performed at 420 nm using a Brinkman PC800 probe colorimeter equipped with a 2 cm path length fiber optic probe. A turbidimetric "type 1" titration (33) was carried out by adding 60 mM SDS in 0.5 M NaCl to a solution of TX100 and QPVP with initial concentrations of 20 mM and 1 g/L, respectively, also in 0.5 M NaCl.

**QPVP Adsorption on CPG.** Four milliliters of QPVP (0.5–20 g/L) in NaCl (0.01–4 M) adjusted to pH 9.5 were added to 0.3 g of CPG. To follow adsorption kinetics, samples were rocked for times varying between 0.5 h and 6 days; otherwise the equilibration time was 4 days. After centrifugation (3000 rpm, 20 min), the supernatant was separated, and the concentration of QPVP was determined by UV spectrophotometry (256 nm) via a standard calibration curve. The CPG–QPVP complexes were washed with 4 mL of Milli-Q water and measurement of the supernatant repeated. The amount of QPVP adsorbed (i.e., retained after washing) per unit surface area ( $\Gamma$ ) was calculated.

To determine whether pollutants might be bound to adsorbed QPVP, toluene (100 ppm) was added to CPG preloaded with 1 and 2.5 g/L QPVP. Samples were rocked overnight, centrifuged (3000 rpm, 20 min), and the supernatants were separated. No significant changes in the UV spectra were observed indicating no toluene uptake by the polymer.

**Micelle Adsorption on CPG–QPVP.** Four milliliters of TX100/SDS ( $Y = [\text{SDS}]/([\text{SDS}] + [\text{TX100}]) = 0.35$ , 20 mM total surfactant concentration, NaCl = 0.5 M, pH 9.5) were added to both untreated CPG and to CPG preloaded with QPVP. The samples were rocked overnight to ensure equilibration. After centrifugation (3000 rpm, 0.5 h), the supernatant was separated, and the concentration of TX100 was measured using a UV calibration curve at 224 nm. The resultant amounts of bound TX100 were calculated and then used to calculate the total mass of micelle bound. The CPG–QPVP–micelle composites "SPIM" were washed with 4 mL of Milli-Q water, the supernatants were measured at 224 nm, and the amounts of micelles remaining bound after washing were calculated. Since our measurement is not sensitive to SDS, a change of  $Y$  upon binding of micelles is of concern.

Penfold et al. studied the adsorption of mixed nonionic/SDS micelles on silica (34). Despite its negative charge (the same sign as silica), SDS adsorbs on silica in the presence of the nonionic surfactant; however, the composition of the mixed micelles does not change at low  $Y$  values. Preferential adsorption of TX100 by silica would result in an increase in  $Y$ , but we found no change in conductivity of the micellar solution (at very low salt concentrations) upon partial binding to porous glass.

### Preparation of SPIMs with Variable Polymer Adsorption.

QPVP (0.5–10 g/L) was added to CPG in 0.5 M NaCl and rocked for 4 days (step 1), followed by the addition of TX100/SDS micelles (step 2) as described above. Excess QPVP (after step 1) and excess micelles (after step 2) were rinsed off as described above. The notation "SPIM2.5", for example, designates 2.5 g/L QPVP in step 1.

**Toluene Uptake by SPIM.** Toluene (14 mL of 100 ppm) was added to SPIM prepared from 0.3 g of CPG as described above with QPVP concentrations from 0.5 to 10 g/L (SPIM0.5–SPIM10). Toluene adsorption isotherms (25–175 ppm) were obtained for SPIM1 and SPIM5, the amount of micelles bound for both being 0.69 mg/g CPG. The SPIM–toluene samples were rocked overnight, centrifuged (3000 rpm, 0.5 h), and the toluene concentrations in the supernatants were measured by HPLC (Beckman, Arlington Heights, IL) equipped with a detector (System Gold 166) set at a wavelength of 254 nm. A reverse phase Phenyl-5PW column (Supelco, Bellefonte, PA) was used. The mobile phase was a mixture of 60% water and 40% acetonitrile. The flow rate was 1 mL/min.

### Halocarbon and Aromatics Mixtures Uptake by SPIM.

Stock standards of 200  $\mu\text{g}/\text{mL}$  pollutants (see Table 1) were diluted to 2000  $\mu\text{g}/\text{L}$  by adding 0.5–0.5 mL of methanol and then bringing the final volume to 50 mL with Milli-Q water. The diluted standard solutions were added to SPIM1 and SPIM5 (20 g/L). The samples were rocked overnight and then centrifuged for 0.5 h at 3000 rpm. The supernatants were diluted by 100 to minimize SDS concentration, which causes problematic foaming. The diluted solutions were then placed in headspace GC/MS vials, accompanied by a diluted stock solution (to measure the actual pollutant concentration). Method 8260B for volatile organic compounds by GC/MS was carried out at Heritage Environmental Services (Indianapolis, IN). The samples were purged and trapped by an OI Eclipse purge Varian Archon autosampler and then transferred to an Agilent 6890 GC and Agilent 5973 mass spectrometer.

## Results and Discussion

**QPVP–Micelle Complexes.** The binding of polyelectrolytes to oppositely charged micelles occurs only when a critical value is attained for the micelle surface charge density which is proportional to the mole fraction of ionic surfactant in the micelle ( $Y$ ). For a given polyelectrolyte–micelle system,  $Y_c$  depends only on ionic strength  $I$  (see ref 33 and others cited therein). Turbidimetric titration (33) (results not shown) was used to confirm a value of  $Y_c = 0.18$ . This is consistent with the value of  $Y_c = 0.18$  at  $I = 0.3$  M (35) for QPVP and dodecyl octa(ethylene glycol)/SDS micelles and shows that the value of  $Y = 0.35$  used in the present study, i.e., well above  $Y_c$ , ensures formation of micelle–polymer complexes.

**QPVP Adsorption on CPG.** The kinetics of QPVP adsorption on CPG are illustrated in Figure 1. The more rapid initial polymer adsorption from higher concentrations, as shown in the inset of Figure 1, is typical for a diffusion-limited process (36).  $\Gamma$ , the amount of QPVP adsorbed per unit surface area, approaches its equilibrium value after 48 h; this  $\Gamma_{\text{equ}}$  increases with concentration. The equilibration time is substantially longer than those typically reported for polymer adsorption on negatively charged surfaces. Such measurements of the time dependence of  $\Gamma$  are generally intended

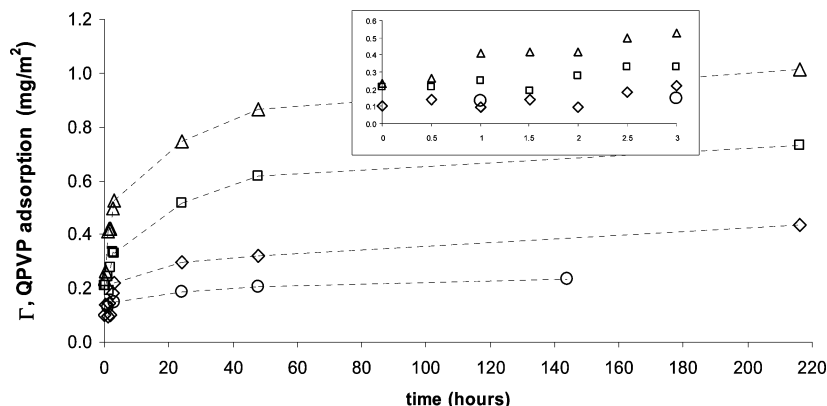


FIGURE 1. QPVP adsorption on CPG at pH 9.5, 0.5 M NaCl, as a function of time for various polymer concentrations: 5 (○), 10 (◇), 15 (□), and 20 (△) g/L. Adsorption for the first 3 h is shown in the inset.

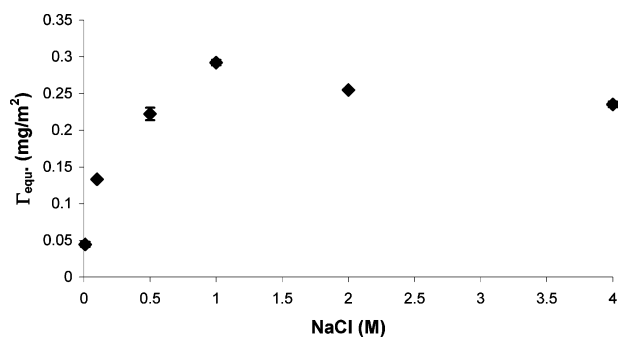


FIGURE 2. Adsorption of QPVP (5 g/L) as a function of ionic strength.

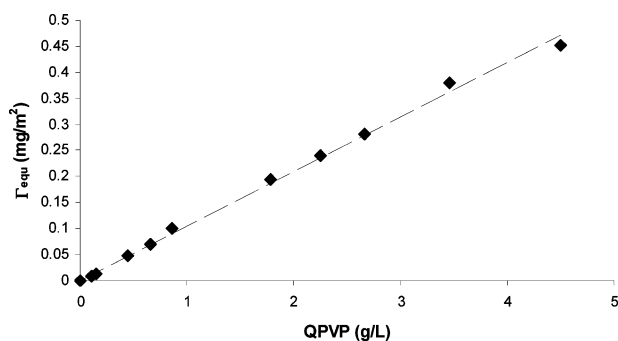


FIGURE 3. QPVP (0–20 g/L, 0.5 M NaCl) adsorption isotherm on CPG.

to determine the time required to reach  $\Gamma_{\text{equ}}$ , usually in the range of seconds to minutes (37). More specifically, equilibrium times of a few minutes have been reported for the adsorption of QPVP (38, 39) and cationic polyacrylamide (36) on nonporous silica and for the adsorption on carboxymethylated cellulosic pulp of 3.6-ionene (40). Assuming the initial adsorption is diffusion-limited, the polymer reaches porous and nonporous surfaces at the same rate, but porous surfaces may provide obstacles to ultimate equilibrium contacts, analogous to the steric barriers discussed by Oedberg et al. (36).

Assuming that equilibrium is reached after 4 days, we determined the ionic strength dependence of  $\Gamma_{\text{equ}}$  at pH = 9.5 (Figure 2). The maximum at  $I = 1$  M agrees with the result for QPVP adsorption on nonporous silica (38). Similar maxima, but at different values of  $I$ , have been observed for other polycation/nonporous surface systems (41), such as QPVP on TiO<sub>2</sub> (39) or cationic polyacrylamide (42), poly-(dimethylaminoethyl methacrylate) (43), and polysine on silica (23). In the low-salt limit corresponding to large Debye lengths, repulsions between adsorbing chains contribute to the adsorption energy and tend to reduce coverage. Increasing salt concentration in the low-salt regime screens these repulsions and increases  $\Gamma_{\text{equ}}$ . Further increases in  $I$  can screen more short-range interactions between polymer segments and the charged surface, and therefore  $\Gamma_{\text{equ}}$  decreases. However, in our case the decrease in  $\Gamma_{\text{equ}}$  at high salt is modest, whereas Sukhishvili and Granick (38) and others show a sharper diminution,  $\Gamma$  going to  $\Gamma_{\text{equ}}$  of nearly zero at  $I$  ca. 4 M.

The dependence of  $\Gamma_{\text{equ}}$  on the concentration of free QPVP shown in Figure 3 is in contrast with typical polymer adsorption isotherms, which reach a plateau (23). Such linearity goes hand-in-hand with the presence of high concentrations of free polymer in equilibrium with adsorbed ones, i.e., a low affinity constant that is also manifested in the delay of the eventual plateau. Alinec et al. (44) also

reported isotherms without plateaus for the adsorption of polyethylenimine on porous pulp fibers even with a specific surface area 3 orders of magnitude lower than that of CPG. Part of their explanation lies in the porosity and swelling properties of the substrate.

Very slow kinetics, linear adsorption isotherms, and the high value of  $\Gamma_{\text{equ}}$  at high  $I$  are not typical for polyelectrolyte adsorption on oppositely charged surfaces. Even more intriguing is the adsorption of QPVP with a hydrodynamic diameter ( $2R_h$ ) (see below) of 12.4 nm on a porous substrate with a pore diameter  $2R_p$  of 7.5 nm. These effects of pore size and ionic strength on polycation adsorption will be the subject of a separate study. However, we would like to point out to the interested reader that QPVP not only can adsorb readily on CPG with  $R_p/R_h < 1$ , but it does so in a manner that provides greater efficiency in micelle binding, and both effects are related to the configurational flexibility of statistical chain polyelectrolytes and the ability in this case for the statistical chain to adopt a configuration with partial confinement of adsorbed segments within the pore. The configurational flexibility of the polymer chain could also explain the slow kinetics of QPVP adsorption on CPG with a small pore size. The kinetics of QPVP adsorption on CPG with a large pore size of 2850 Å (results not shown) were substantially faster (saturation in less than 1 min) than for smaller pore sizes and similar to the adsorption on nonporous silica surfaces noted above. While there are remarkably few reports on polyelectrolyte adsorption kinetics on porous charged surfaces, we suggest that the adsorption of polymers with  $R_p/R_h < 1$  involves first rapid diffusion-controlled binding to the surface, followed by chain reorganization with partial pore penetration. This second step accounts for the slow adsorption seen. Concerning the adsorption isotherm, a typical shape (reaching a plateau) was observed for QPVP on CPG with a large pore size of 2850 Å (results not shown). The partial confinement noted above reduces the number of

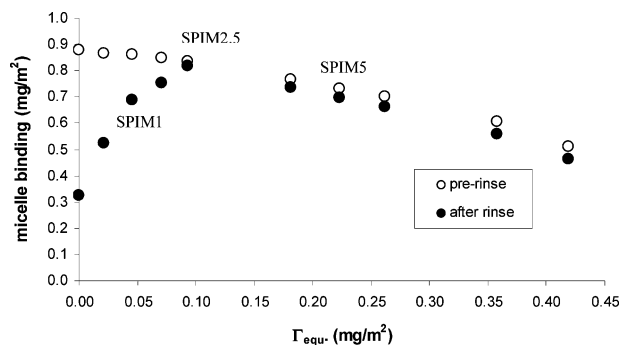


**FIGURE 4.** Micelle (TX100/SDS) binding to CPG preloaded with QPVP. The notation SPIMX designates the concentration of QPVP (g/L) used to coat the CPG prior to subsequent binding of the mixed micelle. The symbols for “pre-rinse” and “after rinse” refer to the condition used to determine the amount of bound micelle.

polycation–glass contacts contributing to the adsorption energy. Shin et al. (45) have discussed how such a reduction leads to a decrease in initial slope with a shift of plateau to higher polymer concentrations. Clearly, this rich phenomenology merits a systematic study of effects of  $R_p/R_h$  and ionic strength, which will appear together with simulations in a separate report.

**Micelle Binding to QPVP–CPG: Effect of SPIM Preparation.** TX100/SDS mixed micelles (20 mM,  $Y = 0.35$ ) were added to both untreated CPG and CPG–QPVP at  $I = 0.5$  and pH 9.5, with the results shown in Figure 4. As expected, micelle binding to CPG first increases with  $\Gamma$  but surprisingly reaches a maximum at  $\Gamma = 0.1$  mg/m<sup>2</sup>. Untreated CPG also completely bound micelles, but two-thirds of that amount was removed by rinsing. For SPIM release of micelles upon rinsing occurred at  $\Gamma < 0.1$  mg/m<sup>2</sup>, but at higher  $\Gamma$  (0.1–0.42 mg/m<sup>2</sup>) nearly no micelles were released. The binding of TX100 to bare silica via H-bonding (34) was apparently only partly suppressed by its incorporation into anionic/nonionic micelles, particularly at high salt. If the removal of mixed micelles by rinsing is attributable to their binding to bare glass, the absence of this effect when  $\Gamma$  exceeds 0.10 mg/m<sup>2</sup> could indicate that no bare glass surface is accessible to the surfactant at higher levels of polymer adsorption.

To elucidate the arrangement of the polymers and micelles on the surface, the CPG area per bound micelle  $100 < A_m < 180$  nm<sup>2</sup> was calculated using a micelle aggregation number of 100 (46). The area per adsorbed polymer chain,  $A_p$ , was calculated from the apparent diameter from DLS of  $D_{app} = 12.4$  nm for QPVP in 0.5 M NaCl, which corresponds to 120 nm<sup>2</sup> for the projected area of a sphere with a radius of 6.3 nm.  $A_p$  was then found to vary from 400 to 8000 nm<sup>2</sup>. These values may be overestimates, since the BET areas refer to all surfaces accessible to N<sub>2</sub>. The large values of  $A_p$  are, however, in agreement with the linear isotherm of Figure 3 and its implication that saturation is not attained. Both results suggest that polymers are not so compressed as to resist further adsorption, perhaps because interpolymer repulsions are suppressed at large  $I$ . For the mixed micelles,  $D_{app} = 24$  nm corresponding to a projected area of 450 nm<sup>2</sup>, larger than the  $A_m$  values noted above. Thus, although the polymer chains are not compressed, the number of micelles per unit surface area of CPG is relatively large. Xia et al. (47) reported a molecular weight of the poly(dimethyldiallylammonium chloride)/TX100/SDS micelle complex an order of magnitude larger than that of the polycation alone, although  $D_{app}$  for the complex was not much larger than  $D_{app}$  of the polymer. Hence, one polymer chain can bind many micelles, i.e., the complex has a high micelle density. The binding of many micelles to each polymer appears to be retained when the polymer is adsorbed.

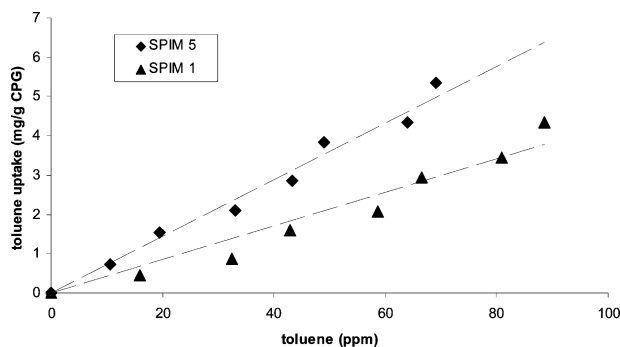


**FIGURE 5.** Toluene uptake vs toluene concentration in equilibrium for SPIM1 and SPIM5.

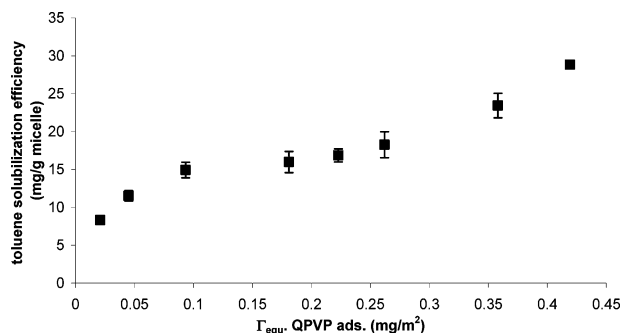


**FIGURE 6.** Solubilization efficiency of toluene by SPIM 0.5–10 as a function of  $\Gamma_{equ}$ .

The maximum in micelle binding with  $\Gamma$  in Figure 4 may be considered in terms of the bound polymer configuration. In general, the configuration of highly charged polyelectrolytes adsorbed on highly charged surfaces is thought to be primarily as “trains”, although loops are more likely to appear in high salt. The loss in solution-state configurational entropy is compensated for by strong electrostatic segmental binding energy (41, 45). Adsorption of polymer within a (small) pore would entail an additional loss of entropy from polymer chain confinement. On the other hand, confinement enhances the number of segment–glass interactions, compensating to some extent for the entropy loss. Our results suggest a bound state in which polymer is partially confined with the pore, leaving an array of unconfined segments accessible. At QPVP loadings of  $\Gamma < 0.1$  mg/m<sup>2</sup>, the adsorption of micelles and their removal on rinsing indicates their binding to some bare CPG. However, at  $\Gamma = 0.1$  mg/m<sup>2</sup>, corresponding to maximum micelle binding, no surfactant is removed, suggesting that the array of unconfined segments mentioned above becomes a continuous “cloud” to which micelles efficiently bind. At still higher  $\Gamma$  (0.1–0.42 mg/m<sup>2</sup>) more pores are occupied, and the interpolymer repulsion of unconfined segments creates a brushlike polymer layer. The reduced micelle-binding efficiency of these stretched chains accounts for the decrease in micelle binding at high  $\Gamma$ .

**Toluene Uptake by SPIM.** The uptake of toluene by SPIM1 and SPIM5, shown as isotherms in Figure 5, is linear as it would be for free micelles, implying that the mechanism of toluene uptake is partitioning into the micelles (12–17). SPIM1 has nearly the same amount of surfactant bound as SPIM5 (Figure 4), but surprisingly, the affinity for toluene is higher for SPIM5.

Toluene uptake (100 ppm) by the different SPIMs (SPIM0.5–10) was measured and found not to correlate linearly with amount of surfactant bound. Solubilization efficiency, i.e., toluene uptake divided by the amount of bound surfactant, is plotted versus  $\Gamma$  in Figure 6. We note the marked effects of  $\Gamma$  and amount of bound surfactant on solubilization efficiency: solubilization efficiency almost

**TABLE 1. Reduction in Pollutant Concentration Due to Treatment with SPIM**

| pollutant                 | added ppb | reduced to concentration ppb |       |
|---------------------------|-----------|------------------------------|-------|
|                           |           | SPIM1                        | SPIM5 |
| benzene                   | 880       | 690                          | 530   |
| bromodichloromethane      | 1300      | 940                          | 700   |
| bromoform                 | 1500      | 740                          | 600   |
| carbon tetrachloride      | 460       | 220                          | 160   |
| chlorobenzene             | 970       | 170                          | 430   |
| dibromochloromethane      | 1600      | 960                          | 780   |
| chloroform                | 1100      | 950                          | 700   |
| 1,2-dichlorobenzene       | 930       | 310                          | 130   |
| 1,3-dichlorobenzene       | 750       | 230                          | 100   |
| 1,4-dichlorobenzene       | 790       | 240                          | 120   |
| 1,1-dichloroethane        | 1000      | 860                          | 650   |
| 1,2-dichloroethane        | 1500      | 1300                         | 1100  |
| 1,1-dichloroethene        | 430       | 310                          | 230   |
| trans-1,2-dichloroethene  | 680       | 550                          | 410   |
| 1,2-dichloropropane       | 1300      | 1100                         | 800   |
| ethylbenzene              | 670       | 310                          | 160   |
| methylene chloride        | 1400      | 1400                         | 1100  |
| 1,1,2,2-tetrachloroethane | 1700      | 1000                         | 630   |
| tetrachloroethene         | 450       | 160                          | <100  |
| toluene                   | 820       | 590                          | 430   |
| 1,1,1-trichloroethane     | 620       | 410                          | 290   |
| 1,1,2-trichloroethane     | 1700      | 1200                         | 1000  |
| trichloroethene           | 890       | 600                          | 420   |

doubles when  $\Gamma$  increases from 0.01 to 0.1 mg/m<sup>2</sup> and nearly doubles again when  $\Gamma$  increases from 0.25 to 0.45 mg/m<sup>2</sup>. In this third region, the apparent area per bound polycation falls from 800 to 400 nm<sup>2</sup>. As mentioned above, the micelle binding values at high  $\Gamma$  suggest that the polymer layer is brushlike, while in the intermediate concentration range polymer chains may approach each other, with possibly overlapping radial segment distributions in a semi-mushroom configuration. If the configurations of the bound polymer change with  $\Gamma$ , then it is appropriate to consider how this might affect the structure and properties of the subsequently polymer-bound micelles.

There are several ways in which micelles bound to polycations in the brush configuration at high  $\Gamma$  could differ from those bound to more solution-like chains: (1) Mixed micelles, whose dimensions are large (>10 nm) compared to interpolymer separations at high  $\Gamma$  may be constrained to brush surfaces. These would be more accessible to toluene than micelles at lower  $\Gamma$  buried in a polymer layer that resides closer to the glass surface. (2) Polarization of micelles (migration of SDS) is more favored for brush-bound micelles leading to the exposure of a nonionic/aromatic-rich palisade layer for toluene solubilization. (3) Toluene solubilization may go together with micelle swelling, so the reduction of steric constraints for the brush-bound micelles could promote solubilization efficiency. We have shown that SDS/TX100 micelles swell upon toluene solubilization (48). This supports explanation 3 for the increase in solubilization efficiency seen at high  $\Gamma$ . The unexpectedly high solubilization efficiency found for SPIM10 is clearly relevant to optimal use of such silica-polycation-micelle systems for remediation, so a more comprehensive understanding of this complex system is worth pursuing.

#### Halocarbon and Aromatics Mixtures Uptake by SPIM.

The reductions in pollutant concentration due to treatment with SPIM1 and SPIM5 are shown in Table 1. These results indicate that SPIM is capable of treating simultaneously a wide range of pollutants and at the low concentrations (ppb) which are relevant to water treatment. SPIM5 has a higher affinity to most of the pollutants than SPIM1 with notable uptake of 20–87%. The higher affinity to SPIM5 for toluene was noted above. In general, the affinity for aromatic pollutants (especially dichlorobenzenes) is higher than that

for halocarbons. The difference in these affinities may be related to the compatibility of the micelle and pollutant molecular structures. However, although a number of studies have attempted to account for the roles of hydrogen bonding, specific solute-headgroup interactions, along with, of course, hydrophobic effects (11, 12, 49, 50), no universal rules have emerged; and the situation is even less understood for competition and solubilization selectivity as embodied in the results of Table 1. Indeed, Guha et al. (49) concluded that single-component partitioning coefficients cannot be used to predict multicomponent micellar solubilization and that both enhancement and suppression can occur in cosolubilization. While it is likely that interference and selectivity for the SPIM materials parallel the behavior of SDS/TX100, even that more fundamental issue has not been satisfactorily addressed.

Full-scale implementation of the SPIM approach would involve both engineering and economic considerations. The current work is based on batch experiments, and evaluation under flow would be a logical next step. Capacity and affinity may be enhanced in combination with other materials, either as PRBs or in sequential filtration. The cost benefit would obviously be improved by replacing the current CPG model system with sand. As shown in a previous study (32), QPVP could be readily replaced with poly(dimethyldiallylammonium chloride) (PDADMAC), an inexpensive and extensively used water-treatment polymer. Also, many anionic/nonionic surfactant systems could be identified that are less expensive than SDS/TX100. These studies should be conducted at lab scale-up levels prior to actual field trials.

#### Acknowledgments

Support from the Israeli Council for Higher Education, Bekura postdoctoral fellowship, is acknowledged.

#### Literature Cited

- (1) Davis, G. B.; Patterson, B. M. Developments in permeable reactive barrier technology. *Biorem.: Crit. Rev.* **2003**, 205–226.
- (2) Scherer, M. M.; Richter, S.; Valentine, R. L.; Alvarez, P. J. J. Chemistry and microbiology of permeable reactive barriers for in situ groundwater clean up. *Crit. Rev. Microbiol.* **2000**, 26, 221–264.
- (3) Birke, V.; Burmeier, H.; Rosenau, D. *Permeable reactive barriers (PRBs) in Germany and Austria: state-of-the-art report 2003*; Department of Civil Engineering (Water and Environmental Management), Coordination Group of RUBIN (German PRB network); University of Applied Sciences-NE Lower Saxony: Gehrden, Germany, 2003.
- (4) O'Hannesin, S. *10 Years of North American experience in granular iron PRB technology for VOC groundwater remediation*; EnviroMetal Technologies, Inc.: Waterloo, ON, Canada, 2003.
- (5) Smith, J.; Boshoff, G.; Bone, B. *Good practice guidance on the use of permeable reactive barriers for remediating polluted groundwater, and a review of their use in the British Isles*; National Groundwater & Contaminated Land Centre, Environmental Agency: Solihull, U.K., 2003.
- (6) Vilensky, M. Y.; Berkowitz, B.; Warshawsky, A. In Situ Remediation of Groundwater Contaminated by Heavy- and Transition-Metal Ions by Selective Ion-Exchange Methods. *Environ. Sci. Technol.* **2002**, 36, 1851–1855.
- (7) Wagner, J.; Chen, H.; Brownawell, B. J.; Westall, J. C. Use of cationic surfactants to modify soil surfaces to promote sorption and retard migration of hydrophobic organic compounds. *Environ. Sci. Technol.* **1994**, 28, 231–237.
- (8) Smith, J. A.; Galan, A. Sorption of Nonionic Organic Contaminants to Single and Dual Organic Cation Bentonites from Water. *Environ. Sci. Technol.* **1995**, 29, 685–692.
- (9) Huttenloch, P.; Roehl, K. E.; Czurda, K. Sorption of Nonpolar Aromatic Contaminants by Chlorosilane Surface Modified Natural Minerals. *Environ. Sci. Technol.* **2001**, 35, 4260–4264.
- (10) Bryant, D. E.; Stewart, D. I.; Kee, T. P.; Barton, C. S. Development of a Functionalized Polymer-Coated Silica for the Removal of Uranium from Groundwater. *Environ. Sci. Technol.* **2003**, 37, 4011–4016.

- (11) Polubesova, T.; Nir, S.; Zadaka, D.; Rabinovitz, O.; Serban, C.; Groisman, L.; Rubin, B. Water Purification from Organic Pollutants by Optimized Micelle-Clay Systems. *Environ. Sci. Technol.* **2005**, *39*, 2343–2348.
- (12) Diallo, M. S.; Abriola, L. M.; Weber, W. J., Jr. Solubilization of Nonaqueous Phase Liquid Hydrocarbons in Micellar Solutions of Dodecyl Alcohol Ethoxylates. *Environ. Sci. Technol.* **1994**, *28*, 1829–1837.
- (13) Pennell, K. D.; Adinolfi, A. M.; Abriola, L. M.; Diallo, M. S. Solubilization of Dodecane, Tetrachloroethylene, and 1,2-Dichlorobenzene in Micellar Solutions of Ethoxylated Nonionic Surfactants. *Environ. Sci. Technol.* **1997**, *31*, 1382–1389.
- (14) Zimmerman, J. B.; Kibbey, T. C. G.; Cowell, M. A.; Hayes, K. F. Partitioning of Ethoxylated Nonionic Surfactants into Nonaqueous-Phase Organic Liquids: Influence on Solubilization Behavior. *Environ. Sci. Technol.* **1999**, *33*, 169–176.
- (15) Cowell, M. A.; Kibbey, T. C. G.; Zimmerman, J. B.; Hayes, K. F. Partitioning of Ethoxylated Nonionic Surfactants in Water/NAPL Systems: Effects of Surfactant and NAPL Properties. *Environ. Sci. Technol.* **2000**, *34*, 1583–1588.
- (16) Liu, G. G.; Roy, D.; Rosen, M. J. A Simple Method To Estimate the Surfactant Micelle-Water Distribution Coefficients of Aromatic Hydrocarbons. *Langmuir* **2000**, *16*, 3595–3605.
- (17) Hill, A. J.; Ghoshal, S. Micellar Solubilization of Naphthalene and Phenanthrene from Nonaqueous-Phase Liquids. *Environ. Sci. Technol.* **2002**, *36*, 3901–3907.
- (18) Fillipi, B. R.; Brant, L. W.; Scamehorn, J. F.; Christian, S. D. Use of Micellar-Enhanced Ultrafiltration at Low Surfactant Concentrations and with Anionic-Nonionic Surfactant Mixtures. *J. Colloid Interface Sci.* **1999**, *213*, 68–80.
- (19) Komesvarakul, N.; Scamehorn, J. F.; Gecol, H. Purification of phenolic-laden wastewater from the pulp and paper industry by using colloid-enhanced ultrafiltration. *Sep. Sci. Technol.* **2003**, *38*, 2465–2501.
- (20) West, C. C.; Harwell, J. H. Surfactants and subsurface remediation. *Environ. Sci. Technol.* **1992**, *26*, 2324–2330.
- (21) Jafvert, C. T. Surfactants and Cosolvents, Purdue University, 1996.
- (22) Harwell, J. H.; Sabatini, D. A.; Knox, R. C. Surfactants for ground water remediation. *Colloids Surf., A* **1999**, *151*, 255–268.
- (23) Cohen-Stuart, M. A.; Fleer, G. J.; Lyklema, J.; Norde, W.; Scheutjens, J. M. H. M. Adsorption of ions, polyelectrolytes and proteins. *Adv. Colloid Interface Sci.* **1991**, *34*, 477–535.
- (24) Kwak, J. C. T., Ed. In *Polymer-Surfactant Systems*; Surfactant Science Series 77, 1998.
- (25) Swanson-Vethamuthu, M.; Dubin, P. L.; Almgren, M.; Li, Y. Cryo-TEM of polyelectrolyte-micelle complexes. *J. Colloid Interface Sci.* **1997**, *186*, 414–419.
- (26) Sudbeck, E. A.; Dubin, P. L.; Curran, M. E.; Skelton, J. Dye solubilization in polyelectrolyte-micelle complexes. *J. Colloid Interface Sci.* **1991**, *142*, 512–517.
- (27) Torn, L. H.; De Keizer, A.; Koopal, L. K.; Lyklema, J. Titration microcalorimetry of poly(vinylpyrrolidone) and sodium dodecylbenzenesulphonate in aqueous solutions. *Colloids Surf., A* **1999**, *160*, 237–246.
- (28) Penfold, J.; Tucker, I.; Staples, E.; Thomas, R. K. Manipulation of the Adsorption of Ionic Surfactants onto Hydrophilic Silica Using Polyelectrolytes. *Langmuir* **2004**, *20*, 7177–7182.
- (29) Roques-Carnes, T.; Aouadj, S.; Filiatre, C.; Membrey, F.; Foissy, A. Interaction between poly(vinylimidazole) and sodium dodecyl sulfate: Binding and adsorption properties at the silica/water interface. *J. Colloid Interface Sci.* **2004**, *274*, 421–432.
- (30) Aloulou, F.; Boufi, S.; Beneventi, D. Adsorption of organic compounds onto polyelectrolyte immobilized-surfactant aggregates on cellulosic fibers. *J. Colloid Interface Sci.* **2004**, *280*, 350–358.
- (31) Wang, Y.; Dubin, P. L. Protein binding on polyelectrolyte-treated glass. Effect of structure of adsorbed polyelectrolyte. *J. Chromatogr., A* **1998**, *808*, 61–70.
- (32) Wang, Y.; Banziger, J.; Dubin, P. L.; Filippelli, G.; Nuraje, N. Adsorptive Partitioning of an Organic Compound onto Polyelectrolyte-Immobilized Micelles on Porous Glass and Sand. *Environ. Sci. Technol.* **2001**, *35*, 2608–2611.
- (33) Wang, Y.; Kimura, K.; Dubin, P. L.; Jaeger, W. Polyelectrolyte-Micelle Coacervation: Effects of Micelle Surface Charge Density, Polymer Molecular Weight, and Polymer/Surfactant Ratio. *Macromolecules* **2000**, *33*, 3324–3331.
- (34) Penfold, J.; Staples, E.; Tucker, I.; Thomas, R. K. Adsorption of mixed anionic and nonionic surfactants at the hydrophilic silica surface. *Langmuir* **2002**, *18*, 5755–5760.
- (35) Hashidzume, A.; Yoshida, K.; Morishima, Y.; Dubin, P. L. Steady-State and Time-Dependent Fluorescence Quenching Studies of the Binding of Anionic Micelles to Polycations. *J. Phys. Chem. A* **2002**, *106*, 2007–2013.
- (36) Oedberg, L.; Sandberg, S.; Welin-Klintstroem, S.; Arwin, H. Thickness of Adsorbed Layers of High Molecular Weight Polyelectrolytes Studied by Ellipsometry. *Langmuir* **1995**, *11*, 2621–2625.
- (37) Pefferkorn, E.; Carroy, A.; Varoqui, R. Adsorption of polyacrylamide on solid surfaces. Kinetics of the establishment of adsorption equilibrium. *Macromolecules* **1985**, *18*, 2252–2258.
- (38) Sukhishvili, S. A.; Granick, S. Polyelectrolyte adsorption onto an initially bare solid surface of opposite electrical charge. *J. Chem. Phys.* **1998**, *109*, 6861–6868.
- (39) Hoogeveen, N. G.; Stuart, M. A. C.; Fleer, G. J. Polyelectrolyte adsorption on oxides. I. Kinetics and adsorbed amounts. *J. Colloid Interface Sci.* **1996**, *182*, 133–145.
- (40) Waagberg, L.; Oedberg, L.; Lindstroem, T.; Aksberg, R. Kinetics of adsorption and ion-exchange reactions during adsorption of cationic polyelectrolytes onto cellulosic fibers. *Colloids Surf.* **1988**, *31*, 119–124.
- (41) Van de Steeg, H. G. M.; Cohen Stuart, M. A.; De Keizer, A.; Bijsterbosch, B. H. Polyelectrolyte adsorption: a subtle balance of forces. *Langmuir* **1992**, *8*, 2538–2546.
- (42) Shubin, V.; Linse, P. Effect of Electrolytes on Adsorption of Cationic Polyacrylamide on Silica: Ellipsometric Study and Theoretical Modeling. *J. Phys. Chem.* **1995**, *99*, 1285–1291.
- (43) Hansupalak, N.; Santore, M. M. Sharp Polyelectrolyte Adsorption Cutoff Induced by a Monovalent Salt. *Langmuir* **2003**, *19*, 7423–7426.
- (44) Alinec, B.; Vanerek, A.; van de Ven, T. G. M. Effects of surface topography, pH and salt on the adsorption of polydisperse polyethylenimine onto pulp fibers. *Ber. Bunsen-Ges.* **1996**, *100*, 954–962.
- (45) Shin, Y.; Roberts, J. E.; Santore, M. M. Influence of charge density and coverage on bound fraction for a weakly cationic polyelectrolyte adsorbing onto silica. *Macromolecules* **2002**, *35*, 4090–4095.
- (46) Lang, J. Surfactant aggregation number and polydispersity of SDS + 1-pentanol mixed micelles in brine determined by time-resolved fluorescence quenching. *J. Phys. Chem.* **1990**, *94*, 3734–3739.
- (47) Xia, J.; Zhang, H.; Rigsbee, D. R.; Dubin, P. L.; Shaikh, T. Structural elucidation of soluble polyelectrolyte-micelle complexes: intravol interpolymer association. *Macromolecules* **1993**, *26*, 2759–2766.
- (48) Mishael, Y. G.; Dubin, P. L. Toluene Solubilization Induces Different Modes of Mixed Micelle Growth. *Langmuir*, published online June 3, <http://dx.doi.org/10.1021/la050513p>.
- (49) Guha, S.; Jaffe, P. R.; Peters, C. A. Solubilization of PAH Mixtures by a Nonionic Surfactant. *Environ. Sci. Technol.* **1998**, *32*, 930–935.
- (50) Rodrigues, M. A.; Alonso, E. O.; Yihwa, C.; Farah, J. P. S.; Quina, F. H. A Linear Solvation Free Energy Relationship Analysis of Solubilization in Mixed Cationic-Nonionic Micelles. *Langmuir* **1999**, *15*, 6770–6774.

Received for review April 20, 2005. Revised manuscript received July 22, 2005. Accepted July 25, 2005.

ES050763S